

*A Stochastic Covariance Shrinkage Approach in
Ensemble Transform Kalman Filtering*

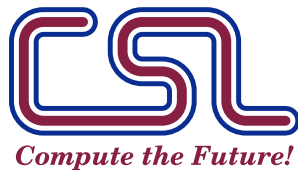
Andrey A Popov, Adrian Sandu, Elias D. Nino-Ruiz, Geir
Evensen

Computational Science Laboratory Report
CSL-TR-20-3
February 17, 2021

Computational Science Laboratory
“Compute the Future!”

Department of Computer Science
Virginia Polytechnic Institute and State University
Blacksburg, VA 24060
Phone: (540)-231-2193
Fax: (540)-231-6075

Email: apopov@vt.edu, sandu@cs.vt.edu, enino@uninorte.edu.co, geev@norceresearch.no
Web: <http://cs1.cs.vt.edu>



A Stochastic Covariance Shrinkage Approach in Ensemble Transform Kalman Filtering

Andrey A Popov* and Adrian Sandu†

Computational Science Laboratory, Department of Computer Science, Virginia Tech

Elias D. Nino-Ruiz‡

Applied Math and Computer Science Lab, Universidad del Norte, Colombia

Geir Evensen§

NORCE and Nansen Environmental and Remote Sensing Center, Norway

(Dated: February 17, 2021)

The Ensemble Kalman Filters (EnKF) employ a Monte-Carlo approach to represent covariance information, and are affected by sampling errors in operational settings where the number of model realizations is much smaller than the model state dimension. To alleviate the effects of these errors EnKF relies on model-specific heuristics such as covariance localization, which takes advantage of the spatial locality of correlations among the model variables. This work proposes an approach to alleviate sampling errors that utilizes a locally averaged-in-time dynamics of the model, described in terms of a climatological covariance of the dynamical system. We use this covariance as the target matrix in covariance shrinkage methods, and develop a stochastic covariance shrinkage approach where synthetic ensemble members are drawn to enrich both the ensemble subspace and the ensemble transformation.

1. INTRODUCTION

The ensemble Kalman filter [5, 11, 12], one of the most widely applied data assimilation algorithms [4, 22, 33], uses a Monte Carlo approach to provide a non-linear approximation to the Kalman filter [20]. In the typical case of an undersampled ensemble the algorithm requires correction procedures such as inflation [1], localization [2, 17, 27, 29, 30, 40], and ensemble subspace enrichment [26, 28, 35].

Hybrid data assimilation [16] is typically an umbrella term for assimilation techniques that combine both offline-estimated climatological covariances with their online-estimated statistical counterparts. These methods are often thought of as heuristic corrections, but in fact stem from statistically rigorous covariance shrinkage techniques.

This work is based on enriching the ensemble subspace through the use of climatological covariances. Previous work [26, 28] proposed augmenting the covariance estimates derived from the ensemble by a full rank shrinkage covariance matrix approximation. In this work we consider augmenting the physical ensemble with synthetic members drawn from a normal distribution with a possibly low rank covariance matrix derived from *a priori* information such as climatological information or method of snapshots. We show that this is equivalent to a stochastic implementation of the shrinkage covariance matrix estimate proposed in [26, 28], and therefore augmenting the physical ensemble with synthetic members enriches the rank of the covariance matrix, and nudges the resulting covariance estimate toward the true covariance.

2. BACKGROUND

Our aim is to understand the behavior of an evolving natural phenomenon. The evolution of the natural phenomenon is approximated by an imperfect dynamical model

$$X_i = \mathcal{M}_{(i-1) \rightarrow i}(X_{i-1}) + \Xi_i, \quad (2.1)$$

where X_{i-1} is a random variable (RV) whose distribution represents our uncertainty in the state of the system at time $i - 1$, $\mathcal{M}_{(i-1) \rightarrow i}$ is the (imperfect) dynamical model, Ξ_i is a RV whose distribution represents our uncertainty in

* apopov@vt.edu

† sandu@cs.vt.edu

‡ enino@uninorte.edu.co

§ geev@norceresearch.no

the additive modeling error, and X_i is the RV whose distribution represents our uncertainty in the (forecasted) state at time i .

One collects noisy observations of the truth:

$$\mathbf{y}_i^o = \mathcal{H}_i(\mathbf{x}_i^t) + \boldsymbol{\eta}_i, \quad (2.2)$$

where \mathbf{x}^t represents the true state of nature represented in model space, \mathcal{H}_i is the (potentially non-linear) observation operator, $\boldsymbol{\eta}_i$ is a RV whose distribution represents our uncertainty in the observations, and \mathbf{y}_i^o are the observation values, assumed to be realizations of an observation RV Y_i . Take n to be the dimension of the state-space, and m to be the dimension of the observation space.

The goal of data assimilation is to find the *a posteriori* estimate of the state given the observations, which is typically achieved through Bayes' theorem. At time i we have:

$$\pi(X_i|Y_i) \propto \pi(Y_i|X_i) \pi(X_i). \quad (2.3)$$

In typical Kalman filtering the assumption of Gaussianity is made, whereby the states at all times, as well as the additive model and observation errors, are assumed to be Gaussian and independently distributed. Specifically one assumes $\Xi_i \sim \mathcal{N}(\mathbf{0}, \mathbf{Q}_i)$ and $\boldsymbol{\eta}_i \sim \mathcal{N}(\mathbf{0}, \mathbf{R}_i)$.

In what follows we use the following notation. The *a priori* estimates at all times are represented with the superscript \square^f , for forecast (as from the imperfect model), and the *a posteriori* estimates are represented with the superscript \square^a , for analysis (through a DA algorithm).

2.1. Ensemble Transform Kalman Filter

Forecasting with an ensemble of coarse models has proven to be a more robust methodology than forecasting with a single fine model [21]. Ensemble Kalman filtering aims to utilize the ensemble of forecasted states to construct empirical moments and use them to implement the Kalman filter formula. The Ensemble Transform Kalman Filter (ETKF) computes an optimal transform of the prior ensemble member states to the posterior member states; for Gaussian distributions the optimal transform is described by a symmetric transform matrix.

We now describe the standard ETKF. Let $\mathbf{X}_{i-1}^a = [\mathbf{x}_{i-1}^{(1),a}, \dots, \mathbf{x}_{i-1}^{(N),a}]$ represent the N -members analysis ensemble at time $i - 1$. The forecast step is:

$$\mathbf{x}_i^{(k),f} = \mathcal{M}_{(i-1) \rightarrow i}(\mathbf{x}_{i-1}^{(k),a}) + \boldsymbol{\xi}_i^{(k)}, \quad k = 1, \dots, N, \quad (2.4)$$

where $\boldsymbol{\xi}_i^{(k)}$ is a random draw from $\mathcal{N}(\mathbf{0}, \mathbf{Q}_i)$.

The ETKF analysis step reads:

$$\mathbf{A}_i^a = \mathbf{A}_i^f \mathbf{T}_i, \quad (2.5a)$$

$$\bar{\mathbf{x}}^a = \bar{\mathbf{x}}^f + \mathbf{A}_i^a \mathbf{Z}^{a,\top} \mathbf{R}^{-1} \mathbf{d}_i, \quad (2.5b)$$

where

$$\mathbf{T}_i = \left(\mathbf{I} - \mathbf{Z}_i^{f,\top} \mathbf{S}_i^{-1} \mathbf{Z}_i^f \right)^{\frac{1}{2}}, \quad (2.6a)$$

$$\mathbf{S}_i = \mathbf{Z}_i^f \mathbf{Z}_i^{f,\top} + \mathbf{R}_i, \quad (2.6b)$$

$$\mathbf{A}_i^f = \frac{1}{\sqrt{N-1}} \left(\mathbf{X}_i^f - \bar{\mathbf{x}}_i^f \mathbf{1}^\top \right), \quad (2.6c)$$

$$\mathbf{Z}_i^f = \frac{1}{\sqrt{N-1}} \left(\mathcal{H}(\mathbf{X}_i^f) - \overline{\mathcal{H}(\mathbf{X}_i^f)} \mathbf{1}^\top \right), \quad (2.6d)$$

$$\mathbf{d}_i = \mathbf{y}_i^o - \overline{\mathcal{H}(\mathbf{X}_i^f)}, \quad (2.6e)$$

$$\bar{\mathbf{x}}_i^f = \frac{1}{N} \sum_{k=1}^N \mathbf{x}_i^{f,(k)}, \quad (2.6f)$$

$$\overline{\mathcal{H}(\mathbf{X}_i^f)} = \frac{1}{N} \sum_{k=1}^N \mathcal{H}(\mathbf{x}_i^{f,(k)}). \quad (2.6g)$$

Here the unique symmetric square root of the matrix is used, as there is evidence of that option being the most numerically stable [37]. Also, it is common practice to approximate \mathbf{Z}^a by

$$\mathbf{Z}^a \approx \mathbf{Z}^f \mathbf{T}_i, \quad (2.7)$$

although in reality \mathbf{Z}^a is implicitly defined from the analysis ensemble \mathbf{X}^a as follows:

$$\begin{aligned} \mathbf{X}_i^a &= \bar{\mathbf{x}}_i^a \mathbf{1}^\top + \sqrt{N-1} \mathbf{A}_i^a, \\ \mathbf{Z}^a &= \frac{1}{\sqrt{N-1}} \left(\mathcal{H}(\mathbf{X}^a) - \overline{\mathcal{H}(\mathbf{X}^a)} \mathbf{1}^\top \right). \end{aligned} \quad (2.8)$$

Note that equation (2.8) is automatically satisfied by (2.7) when \mathcal{H} is a linear operator. Additionally, this implicitly defines a fixed point iteration which should converge when the linear operator is sufficiently smooth. In this paper we make the assumption that equation (2.7) is exact.

The empirical forecast covariance estimate

$$\tilde{\Sigma}_{X_i^f X_i^f} = \mathbf{A}_i^f \mathbf{A}_i^{f,\top} \quad (2.9)$$

is not perfect. In order to improve the performance of EnKF, inflation is applied to the ensemble anomalies,

$$\mathbf{A}_i^f \leftarrow \alpha \mathbf{A}_i^f, \quad (2.10)$$

before any other computation is performed (meaning that it is also applied to the observation anomalies, \mathbf{Z}_i^f as well). The inflation parameter $\alpha > 1$ is typically chosen in a heuristic manner.

2.2. Covariance localization

Traditional state-space localization of the empirical covariance (2.9) is done by tapering, i.e., by using a Schur product

$$\mathbf{B}_i^f = \boldsymbol{\rho}_i \circ \tilde{\Sigma}_{X_i^f X_i^f}, \quad (2.11)$$

with the localization matrix $\boldsymbol{\rho}$ contains entries that are progressively smaller as the distance between the corresponding variables increases. Tapering methods for localization can also be thought of as a type of shrinkage [6].

The localized ETKF (LETKF) [17] is a localization approach to the ETKF. The LETKF and its variants are considered to be one of the state-of-the-art EnKF methods. In the state-space approach to the LETKF, each state space variable $[u]_j$ is assimilated independently of all others, with the observation space error covariance inverse replaced by

$$\mathbf{R}_i^{-1} \leftarrow \boldsymbol{\rho}_{i,j} \circ \mathbf{R}_i^{-1}, \quad (2.12)$$

with the matrix $\boldsymbol{\rho}_{i,[j]}$ being a diagonal matrix representing the decorrelation factor between all observation space variables from the j th state space variable. Each diagonal element represents the tapering factor, and is often chosen to be some function of distance from the state-space variable being assimilated to the corresponding observation-space variable. The implicit assumption is that all observations are independent of each other, in both the observation error (\mathbf{R}_i is diagonal), and forecast error ($\mathbf{Z}^f \mathbf{Z}^{f,\top}$ is assumed to be diagonal).

2.3. Covariance shrinkage

In statistical literature [7–9, 23] covariance shrinkage refers to describe the methodology under which a statistical covariance derived from a set of samples is made to approach the “true” covariance from which the set of samples is derived. For the vast majority of statistical applications, there is no additional apriori knowledge about the distribution of the samples, thus assumptions such as Gaussianity and sphericity are made. In data assimilation applications, however, climatological estimates of covariance are extremely commonplace.

Assume that there exists a target covariance matrix \mathcal{P} that represents the *a priori* knowledge about the error spatial correlations. In this paper we focus on an additive shrinkage covariance structure which is a linear combination of

the empirical covariance (2.9) and the target covariance,

$$\mathbf{B}_i^f = \gamma_i \mu_i \mathcal{P} + (1 - \gamma_i) \tilde{\Sigma}_{X_i^f X_i^f}, \quad (2.13)$$

with γ_i representing the shrinkage factor and μ_i representing a scaling factor. By employing a general target matrix \mathcal{P} , a closed-form expression to compute the weight value γ_i is proposed in [39, 41]. In this derivation, weights are computed as follows:

$$\gamma_i = \min \left(\frac{\frac{1}{N^2} \cdot \sum_{k=1}^N \left\| \mathbf{x}_i^{(k),f} - \bar{\mathbf{x}}_i^f \right\|^4 - \frac{1}{N} \cdot \left\| \tilde{\Sigma}_{X_i^f X_i^f} \right\|^2}{\left\| \tilde{\Sigma}_{X_i^f X_i^f} - \mathcal{P} \right\|^2}, 1 \right), \quad (2.14)$$

but as such an estimate is expensive to compute in an operational setting we will settle for a more computationally inexpensive method. No assumptions about the structure of \mathcal{P} are made to compute γ_i . The general form (2.13) can be reduced to a standard form where the target matrix is the (scaled) identity by defining the statistical covariance $\mathcal{C}_i = \mathcal{P}^{-\frac{1}{2}} \tilde{\Sigma}_{X_i^f X_i^f} \mathcal{P}^{-\frac{1}{2}}$. The corresponding scaling factor, μ_i is then the average covariance of \mathcal{C}_i ,

$$\mu_i = \frac{\text{tr}(\mathcal{C}_i)}{n}, \quad (2.15)$$

with the new target $\mu_i \mathbf{I}$ representing a spherical climatological assumption on \mathcal{C}_i .

The choice of γ_i is extremely important. In this paper we focus on the Rao-Blackwellized Ledoit-Wolf (RBLW) estimator [8] (equation (9) in [27]),

$$\gamma_{i,\text{RBLW}} = \min \left[\frac{N-2}{N(N+2)} + \frac{(n+1)N-2}{\hat{U}_i N(N+2)(n-1)}, 1 \right], \quad (2.16)$$

where the sphericity factor

$$\hat{U}_i = \frac{1}{n-1} \left(\frac{n \text{tr}(\mathcal{C}_i^2)}{\text{tr}^2(\mathcal{C}_i)} - 1 \right) \quad (2.17)$$

measures how similar the correlation structures of the sample covariance and target covariance are. Note that if our samples are also used to calculate the sample mean, the effective sample size of the sample covariance is smaller by one, therefore for most practical applications one replaces N by $N-1$ in (2.16).

The RBLW estimator is valid under Gaussian assumptions about the samples from which the sample covariance matrix is derived, however is only considered to be accurate for an oversampled sample covariance matrix.

There are two major issues with the application of the shrinkage estimator in the EnKF, both related to its reliance on the sphericity of \mathcal{C}_i . First, when operating in the undersampled regime $N \ll n$, the estimate \mathcal{C}_i is also undersampled, and the problem of ‘‘spurious correlations’’ will affect the measure of sphericity (2.17). The second related issue regards the climatological estimate \mathcal{P} . Unless the climatological estimate accurately measures the correlation structure of the sample covariance, the shrinkage estimate could potentially be very poor. The long-term accuracy of the climatological estimate to the covariance is thus of great importance.

Note that \mathcal{P} is not required to be invertible. Commonly, a reduced spectral version of \mathcal{P} is known, $\mathcal{P} = \mathcal{U} \mathcal{L} \mathcal{U}^*$, with the \mathcal{L} being a diagonal matrix of $r \ll n$ spectral coefficients, and \mathcal{U} being an $n \times r$ matrix of orthonormal coefficients. The canonical symmetric pseudo-inverse square-root of \mathcal{P} would therefore be $\mathcal{P}^{-\frac{1}{2}} = \mathcal{U} \mathcal{L}^{-\frac{1}{2}} \mathcal{U}^*$. If σ_i is the i -th singular value of $\mathcal{P}^{-1/2} \mathbf{A}^f$, then the traces appearing in (2.17) can be computed as:

$$\text{tr}(\mathcal{C}) = \sum_{i=1}^{N-1} \sigma_i^2, \quad \text{tr}(\mathcal{C}^2) = \sum_{i=1}^{N-1} \sigma_i^4.$$

3. ETKF IMPLEMENTATION WITH STOCHASTIC SHRINKAGE COVARIANCE ESTIMATES

Ensemble methods propagate our uncertainty about the dynamics of the system. Application of Bayes’ rule requires that all available information is used [18]. Therefore, we attempt to use the locally known climatological information in conjunction with our ensemble information. If the dynamical system is locally (in time) stationary, climatologies

about the local time roughly describe a measure of averaged-in-space uncertainty.

Nino-Ruiz and Sandu [26, 28] proposed to replace the empirical covariance in EnKF with a shrinkage covariance estimator (2.13). They showed that this considerably improves the analysis at a modest additional computational cost. Additional, synthetic ensemble members drawn from a normal distribution with covariance \mathbf{B}^f are used to decrease the sampling errors.

In this work we develop an implementation of ETKF with a stochastic shrinkage covariance estimator (2.13). Rather than computing the covariance estimate (2.13), we build a synthetic ensemble by sampling directly from a distribution with covariance $\mu_i \mathcal{P}$. The anomalies of this synthetic ensemble are independent of the anomalies of the forecast EnKF ensemble.

To be specific, let $\mathcal{X}^f \in \mathbb{R}^{n \times M}$ be a synthetic ensemble of M members (as opposed to the dynamic ensemble \mathbf{X}_i^f with N members) drawn from a climatological probability density. We denote the variables related to the synthetic ensemble by calligraphic letters.

A major concern is the choice of distribution. As sampling from the dynamical manifold is impractical, heuristic assumptions are made about the distributions involved. A useful known heuristic is the principle of maximum entropy (PME) [18]. Given the PME, and the assumption that we know both the mean and covariance of our assumed distribution, and the assumption that the dynamics are supported over all of \mathbb{R}^n , there is one standard interpretation of the information contained in the synthetic ensemble \mathcal{X}_i^f . Assuming that the mean and covariance are known information (through sampling), a Gaussian assumption on the synthetic ensemble is warranted,

$$\mathcal{X}_i^f \sim \mathcal{N}(\bar{\mathbf{x}}_i^f, \mu_i \mathcal{P}). \quad (3.1)$$

Alternatively, not explored in this paper, a Laplace assumption on the synthetic ensemble can be assumed. The Laplace assumption has obvious parallels to robust statistics methods in data assimilation [32]. By sampling from a Laplace distribution, outlier behaviour can more readily be captured with fewer samples. However, the concentration of samples around the mean is also increased, thereby requiring more samples to better represent the covariance. The Gaussian assumption appears more natural in Kalman filter-based methods, and thus the rest of the paper will make this assumption.

The synthetic ensemble anomalies in the state and observation spaces are:

$$\begin{aligned} \mathcal{A}_i^f &= \frac{1}{\sqrt{M-1}} \left(\mathcal{X}_i^f - \bar{\mathbf{x}}_i^f \mathbf{1}^\top \right) \in \mathbb{R}^{n \times M}, \\ \mathcal{Z}_i^f &= \frac{1}{\sqrt{M-1}} \left(\mathcal{H}(\mathcal{X}_i^f) - \overline{\mathcal{H}(\mathcal{X}_i^f)} \mathbf{1}^\top \right) \in \mathbb{R}^{m \times M}. \end{aligned} \quad (3.2)$$

The shrinkage estimator (2.13) of the forecast error covariance for \mathbf{B}_i^f is represented in terms of synthetic and forecast anomalies as:

$$\tilde{\mathbf{B}}_i^f = \gamma_i \mathcal{A}_i^f \mathcal{A}_i^{f,\top} + (1 - \gamma_i) \mathbf{A}_i^f \mathbf{A}_i^{f,\top}. \quad (3.3)$$

The Kalman filter formulation [20] yields the following analysis covariance matrix:

$$\tilde{\mathbf{B}}_i^a = \tilde{\mathbf{B}}_i^f - \tilde{\mathbf{B}}_i^f \mathbf{H}_i^\top \mathbf{S}_i^{-1} \mathbf{H}_i \tilde{\mathbf{B}}_i^f, \quad (3.4)$$

where \mathbf{S}_i will be discussed later.

Using the forecast error covariance estimate (3.3) in (3.4) leads to the following analysis covariance:

$$\begin{aligned} \tilde{\mathbf{B}}_i^a &= \gamma_i \mathcal{A}_i^f \mathcal{A}_i^{f,\top} + (1 - \gamma_i) \mathbf{A}_i^f \mathbf{A}_i^{f,\top} \\ &\quad - \left(\gamma_i \mathcal{A}_i^f \mathcal{Z}_i^{f,\top} + (1 - \gamma_i) \mathbf{A}_i^f \mathbf{Z}_i^{f,\top} \right) \mathbf{S}_i^{-1} \left(\gamma_i \mathcal{Z}_i^f \mathcal{A}_i^{f,\top} + (1 - \gamma_i) \mathbf{Z}_i^f \mathbf{A}_i^{f,\top} \right), \end{aligned} \quad (\text{goal-cov})$$

which we refer to as the ‘‘target’’ analysis covariance formula.

The goal of our modified ensemble Kalman filter is to construct an N -member analysis ensemble such that the anomalies \mathbf{A}_i^a (2.5a) represent the (goal-cov) analysis covariance as well as possible:

$$\text{Find } \mathbf{A}_i^a \in \mathbb{R}^{n \times N} \text{ such that : } \mathbf{A}_i^a \mathbf{A}_i^{a,\top} \approx \tilde{\mathbf{B}}_i^a. \quad (\text{goal-an})$$

In the proposed method, we enrich our forecast ensemble in a way that closely approximates the shrinkage covariance (2.13). An alternative approach, where we transform the physical ensemble and the surrogate ensemble as

separate entities that are only related by the common information in their transformations, is discussed in Appendix A.

3.1. The method

We enrich the ensembles of forecast anomalies with synthetic anomalies (3.2):

$$\begin{aligned}\mathcal{A}_i^f &= [\sqrt{1-\gamma_i} \mathbf{A}_i^f \quad \sqrt{\gamma_i} \mathcal{A}_i^f] \in \mathbb{R}^{n \times (N+M)}, \\ \mathcal{Z}_i^f &= [\sqrt{1-\gamma_i} \mathbf{Z}_i^f \quad \sqrt{\gamma_i} \mathcal{Z}_i^f] \in \mathbb{R}^{m \times (N+M)}.\end{aligned}\quad (3.5)$$

Next, we define a transform matrix (2.5a) that is applied to the enriched ensemble (3.5), and leads to an analysis ensemble that represents the target analysis covariance (goal-an). Specifically, we search for a transform matrix \mathcal{T}_i such that:

$$\tilde{\mathbf{B}}_i^a = \mathcal{A}_i^f \mathcal{T}_i \mathcal{T}_i^T \mathcal{A}_i^{f,T}. \quad (3.6)$$

Using the extended ensembles (3.6) the (goal-cov) becomes

$$\tilde{\mathbf{B}}_i^a = \mathcal{A}_i^f \left(\mathbf{I}_{(N+M) \times (N+M)} - \mathcal{Z}_i^{f,T} \mathbf{S}_i^{-1} \mathcal{Z}_i^f \right) \mathcal{A}_i^{f,T}, \quad (3.7)$$

where, from (2.6b),

$$\mathbf{S}_i = \mathcal{Z}_i^f \mathcal{Z}_i^{f,T} + \mathbf{R}_i. \quad (3.8)$$

The transform matrix (2.6a) is a square root of (3.6):

$$\mathcal{T}_i = \left(\mathbf{I}_{(N+M) \times (N+M)} - \mathcal{Z}_i^{f,T} \mathbf{S}_i^{-1} \mathcal{Z}_i^f \right)^{\frac{1}{2}}. \quad (3.9)$$

We compute the analysis mean using the shrinkage covariance estimate. From (2.5b):

$$\bar{\mathbf{x}}_i^a = \bar{\mathbf{x}}_i^f + \mathcal{A}_i^f \mathcal{T}_i \mathcal{T}_i^T \mathcal{Z}_i^{f,T} \mathbf{R}_i^{-1} \mathbf{d}_i, \quad (3.10)$$

where the full analysis covariance estimate (3.7) is used. In addition, we achieve the (goal-an) by keeping the first N members of the transformed extended ensemble, or equivalently, the first N columns of the symmetric square root (3.9). From (2.5a) we have:

$$\mathbf{A}_i^a = \frac{1}{\sqrt{1-\gamma_i}} [\mathcal{A}_i^f \mathcal{T}_i]_{:,1:N} = \frac{1}{\sqrt{1-\gamma_i}} \mathcal{A}_i^f \check{\mathcal{T}}_i, \quad \check{\mathcal{T}}_i = [\mathcal{T}_i]_{:,1:N}. \quad (3.11)$$

An alternative approach to achieve the (goal-an) is to look for a low-rank, approximate square root instead of the symmetric square root (3.9). Specifically, we seek a transformation matrix $\hat{\mathcal{T}}_i$ such that:

$$\hat{\mathcal{T}}_i \in \mathbb{R}^{(N+M) \times N}, \quad \hat{\mathcal{T}}_i \hat{\mathcal{T}}_i^T \approx \mathbf{I}_{(N+M) \times (N+M)} - \mathcal{Z}_i^{f,T} \mathbf{S}_i^{-1} \mathcal{Z}_i^f. \quad (3.12)$$

The calculation of the symmetric square root (3.9) requires an SVD of the right hand side matrix. With the same computational effort one can compute the low rank transformation:

$$\begin{aligned}\mathbf{U} \boldsymbol{\Sigma} \mathbf{U}^T &= \left(\mathbf{I} - \mathcal{Z}_i^{f,T} \mathbf{S}_i^{-1} \mathcal{Z}_i^f \right), \quad \mathbf{U}, \boldsymbol{\Sigma} \in \mathbb{R}^{(N+M) \times (N+M)}, \\ \check{\mathcal{T}}_i &= \mathbf{U} \boldsymbol{\Sigma}^{1/2} [\mathbf{U}_{1:N,:}]^T \in \mathbb{R}^{(N+M) \times N} \quad (\text{symmetric square root (3.9)}); \\ \hat{\mathcal{T}}_i &= \mathbf{U}_{:,1:N} \boldsymbol{\Sigma}_{1:N,1:N}^{1/2} \in \mathbb{R}^{(N+M) \times N} \quad (\text{low rank square root (3.12)}).\end{aligned}\quad (3.13)$$

The mean calculation (3.10) is the same. The ensemble transform produces N transformed ensemble members that contain ‘‘mixed’’ information from both the physical and the synthetic ensembles:

$$\mathbf{A}_i^a = \frac{1}{\sqrt{1-\gamma_i}} \mathcal{A}_i^f \hat{\mathcal{T}}_i.$$

Remark 1 (Classical localization) *It is possible to combine the proposed stochastic shrinkage approach with traditional localization. The LETKF implementation [17] computes transform matrices for subsets of variables, corresponding to localized spatial domains. In a similar vein one can combine our shrinkage algorithm with classical localization, as follows. Subsets of variables of the enriched ensembles (3.5) are used to compute local transform matrices (3.9) or (3.12), which are then applied to transform the corresponding local subsets, i.e. to compute the corresponding rows in equations (3.11) or (3.11), respectively. Insofar, the authors have not observed this to have any measurable effect on the error.*

4. NUMERICAL EXPERIMENTS

All test problem implementations are available in the ‘ODE Test Problems’ suite [10, 34].

4.1. The Lorenz’96 model (L96)

We first consider the 40-variable Lorenz ’96 problem [24],

$$[y]_i' = -[y]_{i-1} ([y]_{i-2} - [y]_{i+1}) - [y]_i + F, \quad i = 1, \dots, 40, \quad F = 8. \quad (4.1)$$

Assuming (4.1) is ergodic (thus having a constant spatio-temporal measure of uncertainty on the manifold of the attractor), we compute the target covariance matrix \mathcal{P} as the empirical covariance from 10,000 independent ensemble members run over 225 days in the system (where 0.05 time units corresponds to 6 hours), with an interval of 6 hours between snapshots. This system is known to have 13 positive Lyapunov exponents, with a Kaplan-Yorke dimension of about 27.1 [31].

The time between consecutive assimilation steps is $\Delta t = 0.05$ units, corresponding to six hours in the system. All variables are observed directly with an observation error covariance matrix of $\mathbf{R}_i = \mathbf{I}_{40}$. The time integration of the model is performed with RK4 the fourth order Runge-Kutta scheme RK4 [14] with a step size $h = \Delta t$. The problem is run over 2200 assimilation steps. The first 200 are discarded to account for model spinup. Twenty independent model realizations are performed in order to glean statistical information thereof.

4.2. L96 assimilation results

We assess the quality of the analysis ensembles using a rank histogram [15], cumulative over 20 independent runs. For a quantitative metric we compute the KL divergence from Q to P ,

$$D_{KL}(P||Q) = -\sum_k P_k \log\left(\frac{P_k}{Q_k}\right), \quad (4.2)$$

where P is the uniform distribution and Q is our ensemble rank histogram, and P_k & Q_k are the discrete probabilities associated with each bin.

Additionally, for testing the accuracy of all our methods we compute the spatio-temporal RMSE,

$$\sqrt{\sum_{i=1}^K \sum_{j=1}^n [x_i]_j^2}, \quad (4.3)$$

with K representing the amount of snapshots at which the analysis is computed, and $[x_i]_j$ is the j th component of the state variable at time i .

For the given settings of a severely undersampled ensemble ($N = 5$) and mild inflation ($\alpha = 1.1$), we compare the Gaussian sampling methodology coupled to the RBLW formulation for the shrinkage factor γ (2.16), with the optimal static $\gamma = 0.85$ shrinkage factor. For a dynamic ensemble that captures the positive error growth modes ($N = 14$) will compare the RBLW estimator with the optimal static $\gamma = 0.1$. We will compare the mean and variance of the KL divergence of the rank histogram of the variable $[y]_{17}$ from the uniform, and the statistics of the spatio-temporal RMSE.

The results are reported in Figure 1. For both an undersampled and sufficient ensemble, the optimal shrinkage factor has a smaller mean error, and a smaller KL divergence with less variance (top left, top middle, bottom left, and

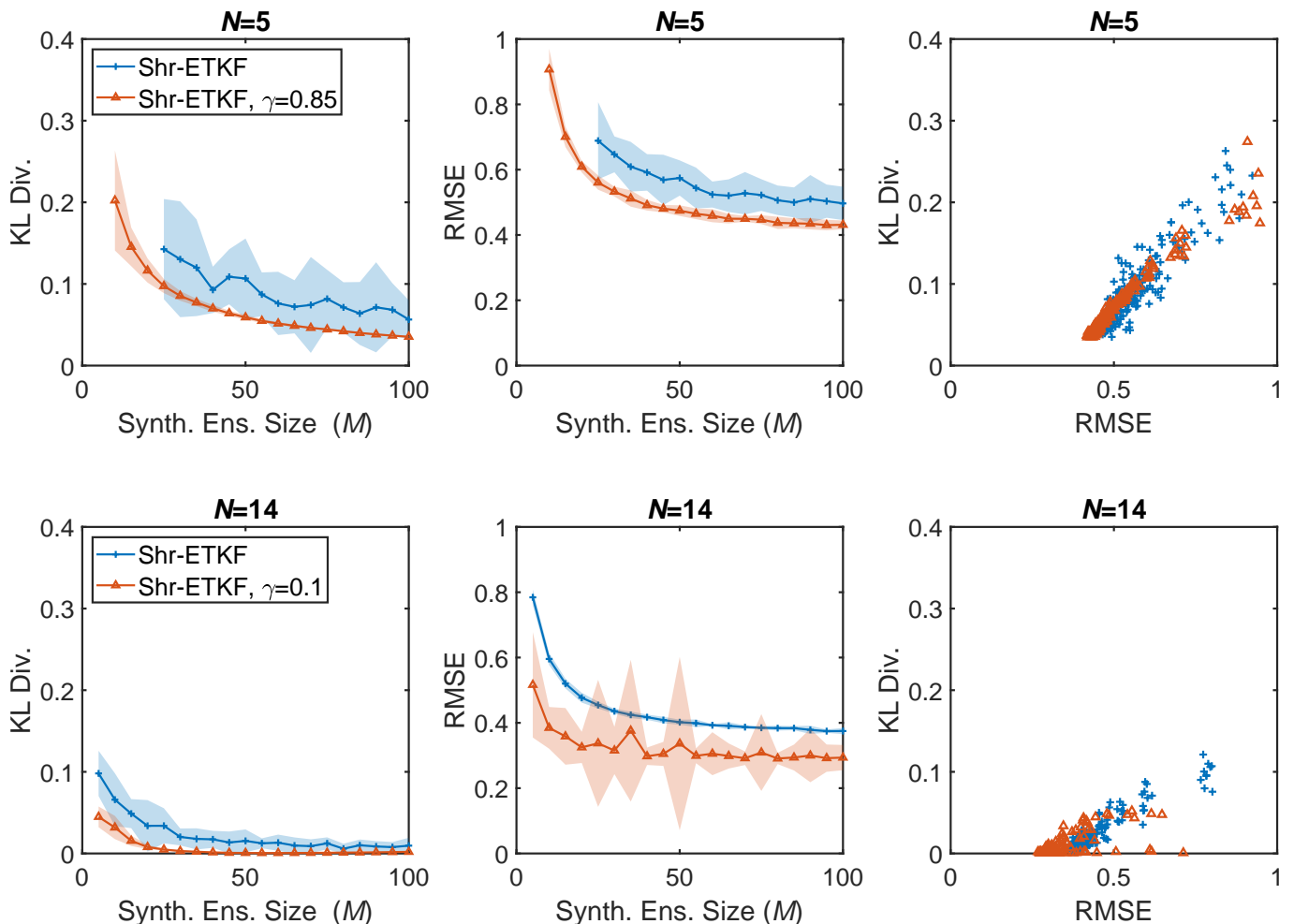


FIG. 1: Results for the L96 problem with dynamic ensemble sizes of $N = 5$ and $N = 14$, inflation factor $\alpha = 1.1$, and different synthetic ensemble sizes M . We compute the KL divergence of the rank histogram (4.2) and the RMSE (4.3) for the methods. Error bars show two standard deviations.

bottom middle panels). In the undersampled case, the RBLW estimator induces more variance into the RMSE (top middle panel). For the sufficiently sampled ensemble, however, the optimal static shrinkage value induced significantly more variance into the error, with the RBLW estimator reducing the error significantly (bottom middle panel).

It is possible that a better estimator than RBLW may get the ‘best of both worlds’ and induce low error with low variance, though this is as-of-yet out of reach. This is to be expected as the RBLW estimate is only accurate in the limit of ensemble size, and there is no theory about its accuracy in the undersampled case. In the authors’ experience other estimators such as OAS, while having the theoretically desired properties, perform empirically worse in conjunction with ensemble methods. Currently, for a modest reduction in accuracy, one of the hyperparameters can be estimated online by the methodology.

For the second round of experiments with Lorenz ’96, reported in Figure 2, we comparing analysis errors when the synthetic and dynamic ensemble sizes are modified (left panel). It is evident that increases in both dynamic and synthetic ensemble size lead to lower error. In the right panel we also compare dynamic ensemble size the values of γ that are produced. It is clear that an increase in dynamic ensemble size decreases the need for shrinkage.

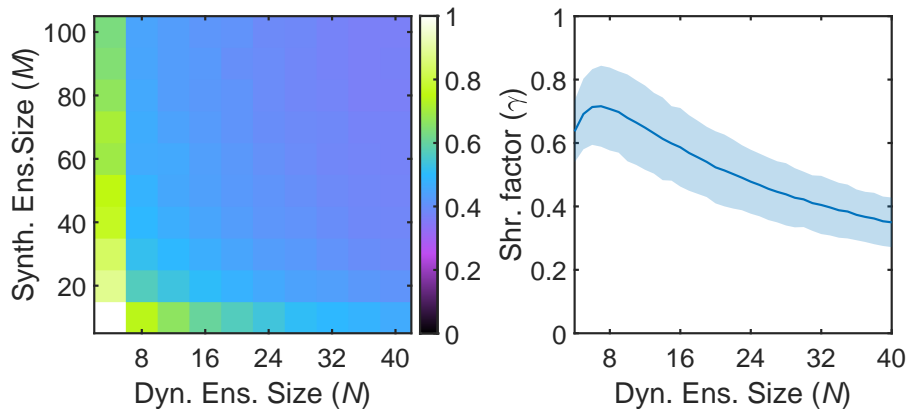


FIG. 2: The left panel presents the RMSE of the L96 model for various values of the dynamic and synthetic ensemble sizes. The right panel presents the shrinkage factor γ for a synthetic ensemble size of $M = 100$, with error bars showing two standard deviations.

4.3. The Quasi-Geostrophic model (QG)

We follow the QG formulations given in [25, 38]. We discretize the equation

$$\begin{aligned} \omega_t + J(\psi, \omega) - Ro^{-1} \psi_x &= Re^{-1} \Delta \omega + Ro^{-1} F, \\ J(\psi, \omega) &\equiv \psi_y \omega_x - \psi_x \omega_y, \end{aligned} \quad (4.4)$$

where ω stands for the vorticity, ψ stands for the stream function, Re is the Reynolds number, Ro is the Rossby number, J is the Jacobian term, and F is a constant (in time) forcing term.

The relationship between stream and vorticity, $\omega = -\Delta \psi$ is explicitly enforced in the evaluation of the ODE. The forcing term is a symmetric double gyre,

$$F = \sin(\pi(y - 1)). \quad (4.5)$$

Homogeneous Dirichlet boundary conditions are enforced on the spatial domain $[0, 1] \times [0, 2]$. The spatial discretization is a second order central finite difference for the first derivatives, and the Laplacian, with the Arakawa approximation [3] (a pseudo finite element scheme [19]) used for computing the Jacobian term. All spatial discretizations exclude the trivial boundary points from explicit computation.

The matrix \mathcal{P} is approximated from 700 snapshots of the solution about 283 hours apart each, with Gaspari-Cohn localization applied, so as to keep the matrix sparse. The true model is run outside of time of the snapshots so as to not pollute the results. Nature utilizes a 255×511 spatial discretization, and the model a 63×127 spatial discretization. Observations are first relaxed into the model space via multigriding [42], then 150 distinct spatial points (using an observation operator similar to [36]) from the non-linear observation operator,

$$\mathcal{H}(\psi) = \sqrt{\psi_x^2 + \psi_y^2}, \quad (4.6)$$

representing zonal wind magnitude, are taken. The observation error is unbiased, with covariance $\mathbf{R} = 4\mathbf{I}_{150}$. The number of synthetic ensemble members is fixed at a constant $M = 100$, as to be more than the number of full model run ensemble members, but significantly less than the rank of the covariance. Observations are taken $\Delta t = 0.010886$ time units (representing one day in model space) apart. We run a total of 350 assimilation steps, taking the first 50 as spinup. Results are averaged over 5 model runs (with the same nature run, but different initializations of the dynamic ensemble), with diverged runs treated as de-facto infinite error.

Operationally, the LETKF assumes that observations are sufficiently far apart that almost no two points are influenced by the same observation, and the algorithm runs on ‘patches’ defined by the observations. In such an operational framework, equation (2.12) cannot be applied. Thus, using an extremely nice decorrelation function such as Gaspari-Cohn [13] (GC) is not operationally feasible. Defining sharp boundaries for the patches would be equally unfair. As such, in addition to looking at the GC decorrelation function, we will construct a decorrelation function

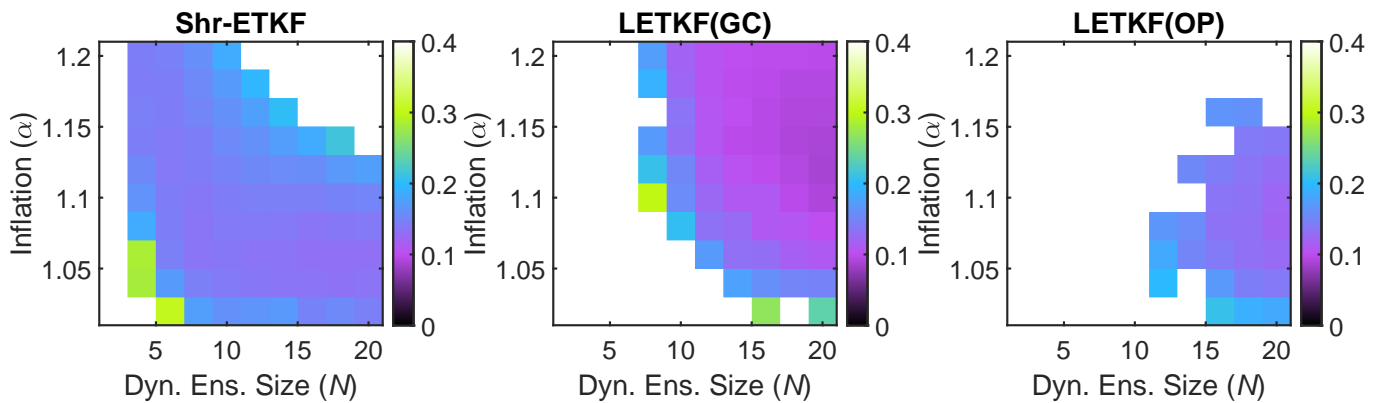


FIG. 3: Analysis RMSE results with the QG equations. For QG, $M = 100$, and Gaussian and Laplace samples, as compared to the LETKF with both the Gaspari-Cohn decorrelation function (GC) and our operational approximation (OP) (4.7).

that has both a built-in cut-off radius, but also allows for a smoother coupling between neighboring patches:

$$\ell(k) = \begin{cases} 1 & k \leq 1 \\ (5 - 4k)^2(8k - 7) & 1 < k \leq \frac{5}{4}, \\ 0 & \text{const.} \end{cases} \quad (4.7)$$

where $k_{ij} = d_{ij}/r$ is the ratio between the distance of two given points and the decorrelation radius (which we will set to 15 grid points). The nonlinear term is an approximation to a sigmoid function.

4.4. QG assimilation results

Figure 3 reports the results with the QG model. The shrinkage approach handily beats the operational approximation decorrelation function (4.7) both in terms of stability and in terms of RMSE for the vast majority of chosen dynamic ensemble size N and inflation factor α . Comparing our methodology to the LETKF with Gaspari-Cohn (GC) localization, we see that GC significantly decreases the error for larger values of N and α , but is not stable for more operational under-sampled dynamic ensemble sizes and low inflation factors, as opposed to our shrinkage method. Possible sources of error are both the nonlinear observations and the coarse approximation to the covariance estimate.

These results lend additional support to the argument that a better (perhaps more heuristic) approximation to the shrinkage factor γ is needed in order to use our methodology coupled with localization to stabilize operational implementations of the LETKF.

The quasi-geostrophic results indicate that our methodology holds promise to be of use for practical data assimilation systems, especially those for which the observations are non-linear transformations of the state representation. However, the methodology needs to be refined with more optimal shrinkage factors for operational undersampled empirical covariances.

Remark 2 *An operational implementation of the LETKF requires $m \times N$ linear solves and m matrix square roots, while our stochastic shrinkage algorithm requires $N + M$ linear solves and one matrix square root. Thus as the number of observations grows, the stochastic shrinkage methodology becomes a lot more compelling.*

5. DISCUSSION

In [26] it was shown that shrinkage covariance matrix estimators can greatly improve the performance of the EnKF. This work develops ensemble transform filters that utilize a stochastic implementation of shrinkage covariance matrix estimates. We compare our filter to the current state-of-the-art LETKF algorithm. Lorenz '96 results indicate that the new filter performs worse in the under-sampled regime than the best 'static' shrinkage method, and performs

better (in terms of less variance in the error) than an optimal dynamic shrinkage method for the sufficiently sampled case. Additional results with QG indicate that our method could potentially be used to augment operational LETKF implementations, but that more work is needed to devise better heuristic estimates of the shrinkage factor γ such that the two approaches could potentially be coupled.

ACKNOWLEDGMENTS

The first two authors would like to thank Traian Iliescu and Changhong Mou for their in-depth help with understanding of the Quasi-Geostrophic model, Steven Roberts, the primary maintainer of the ODE Test Problems package, and the rest of the members of the Computational Science Laboratory at Virginia Tech for their continuous support.

The authors would like to thank Dr. Pavel Sakov and a second, Anonymous, referee for their insightful feedback that lead to an improved paper.

The first two authors were supported, in part, by the National Science Foundation through awards NSF ACI-1709727 and NSF CCF-1613905, AFOSR through the award AFOSR DDDAS 15RT1037, and by DOE ASCR through the award DE-SC0021313.

The last author was supported by the Research Council of Norway and the companies AkerBP, Wintershall-DEA, Vår Energy, Petrobras, Equinor, Lundin and Neptune Energy, through the Petromaks-2 project (280473) DIGIRES (<http://digires.no>)

REFERENCES

-
- [1] Anderson, J. L. (2001). An ensemble adjustment Kalman filter for data assimilation. *Monthly Weather Review*, 129(12):2884–2903.
 - [2] Anderson, J. L. (2012). Localization and sampling error correction in ensemble Kalman filter data assimilation. *Monthly Weather Review*, 140(7):2359–2371.
 - [3] Arakawa, A. (1966). Computational design for long-term numerical integration of the equations of fluid motion: Two-dimensional incompressible flow. Part I. *Journal of Computational Physics*, 1(1):119–143.
 - [4] Asch, M., Bocquet, M., and Nodet, M. (2016). *Data assimilation: methods, algorithms, and applications*. SIAM.
 - [5] Burgers, G., Jan van Leeuwen, P., and Evensen, G. (1998). Analysis scheme in the ensemble kalman filter. *Monthly weather review*, 126(6):1719–1724.
 - [6] Chen, X., Wang, Z. J., and McKeown, M. J. (2012). Shrinkage-to-tapering estimation of large covariance matrices. *IEEE Transactions on Signal Processing*, 60(11):5640–5656.
 - [7] Chen, Y., Wiesel, A., Eldar, Y. C., and Hero, A. O. (2010). Shrinkage algorithms for mmse covariance estimation. *IEEE Transactions on Signal Processing*, 58(10):5016–5029.
 - [8] Chen, Y., Wiesel, A., and Hero, A. O. (2009). Shrinkage estimation of high dimensional covariance matrices. In *2009 IEEE International Conference on Acoustics, Speech and Signal Processing*, pages 2937–2940. IEEE.
 - [9] Chen, Y., Wiesel, A., and Hero, A. O. (2011). Robust shrinkage estimation of high-dimensional covariance matrices. *IEEE Transactions on Signal Processing*, 59(9):4097–4107.
 - [10] Computational Science Laboratory (2020). ODE test problems.
 - [11] Evensen, G. (1994). Sequential data assimilation with a nonlinear quasi-geostrophic model using Monte Carlo methods to forecast error statistics. *Journal of Geophysical Research: Oceans*, 99(C5):10143–10162.
 - [12] Evensen, G. (2009). *Data assimilation: the ensemble Kalman filter*. Springer Science & Business Media.
 - [13] Gaspari, G. and Cohn, S. E. (1999). Construction of correlation functions in two and three dimensions. *Quarterly Journal of the Royal Meteorological Society*, 125(554):723–757.
 - [14] Hairer, E., Nørsett, S. P., and Wanner, G. (1991). *Solving ordinary differential equations. 1, Nonstiff problems*. Springer-Vlg.
 - [15] Hamill, T. M. (2001). Interpretation of rank histograms for verifying ensemble forecasts. *Monthly Weather Review*, 129(3):550–560.
 - [16] Hamill, T. M. and Snyder, C. (2000). A hybrid ensemble Kalman filter–3d variational analysis scheme. *Monthly Weather Review*, 128(8):2905–2919.
 - [17] Hunt, B. R., Kostelich, E. J., and Szunyogh, I. (2007). Efficient data assimilation for spatiotemporal chaos: A local ensemble transform Kalman filter. *Physica D: Nonlinear Phenomena*, 230(1-2):112–126.
 - [18] Jaynes, E. T. (2003). *Probability theory: The logic of science*. Cambridge university press.
 - [19] Jespersen, D. C. (1974). Arakawa’s method is a finite-element method. *Journal of computational physics*, 16(4):383–390.

- [20] Kalman, R. E. (1960). A new approach to linear filtering and prediction problems. *Journal of basic Engineering*, 82(1):35–45.
- [21] Kalnay, E. (2003). *Atmospheric modeling, data assimilation and predictability*. Cambridge university press.
- [22] Law, K., Stuart, A., and Zygalakis, K. (2015). *Data assimilation: a mathematical introduction*, volume 62. Springer.
- [23] Ledoit, O. and Wolf, M. (2004). A well conditioned estimator for large dimensional covariance matrices. *Journal of Multivariate Analysis*, 88(2):365–411.
- [24] Lorenz, E. N. (1996). Predictability: A problem partly solved. In *Proc. Seminar on predictability*, volume 1.
- [25] Mou, C., Liu, H., Wells, D. R., and Iliescu, T. (2019). Data-driven correction reduced order models for the quasi-geostrophic equations: A numerical investigation. *arXiv preprint*, <http://arxiv.org/abs/1908.05297>.
- [26] Nino-Ruiz, E. and Sandu, A. (2015). Ensemble Kalman filter implementations based on shrinkage covariance matrix estimation. *Ocean Dynamics*, 65(11):1423–1439.
- [27] Nino-Ruiz, E. and Sandu, A. (2017). An ensemble Kalman filter implementation based on modified Cholesky decomposition for inverse covariance matrix estimation. *SIAM Journal on Scientific Computing*, submitted.
- [28] Nino-Ruiz, E. and Sandu, A. (2018). Efficient parallel implementation of DDDAS inference using an ensemble Kalman filter with shrinkage covariance matrix estimation. *Cluster Computing*, pages 1–11.
- [29] Nino-Ruiz, E. D., Sandu, A., and Deng, X. (2015). A parallel ensemble Kalman filter implementation based on modified Cholesky decomposition. In *Proceedings of the 6th Workshop on Latest Advances in Scalable Algorithms for Large-Scale Systems*, volume Supercomputing 2015 of *Scala '15*, Austin, Texas.
- [30] Petrie, R. (2008). Localization in the ensemble Kalman filter. *MSc Atmosphere, Ocean and Climate University of Reading*.
- [31] Popov, A. A. and Sandu, A. (2019). A bayesian approach to multivariate adaptive localization in ensemble-based data assimilation with time-dependent extensions. *Nonlinear Processes in Geophysics*, 26(2):109–122.
- [32] Rao, V., Sandu, A., Ng, M., and Nino-Ruiz, E. D. (2017). Robust data assimilation using l1 and huber norms. *SIAM Journal on Scientific Computing*, 39(3):B548–B570.
- [33] Reich, S. and Cotter, C. (2015). *Probabilistic forecasting and Bayesian data assimilation*. Cambridge University Press.
- [34] Roberts, S., Popov, A. A., and Sandu, A. (2019). ODE test problems: a MATLAB suite of initial value problems. *CoRR*, abs/1901.04098.
- [35] Ruiz, E. N., Sandu, A., and Anderson, J. (2014). An efficient implementation of the ensemble Kalman filter based on an iterative Sherman–Morrison formula. *Statistics and Computing*, pages 1–17.
- [36] Sakov, P. and Oke, P. R. (2008a). A deterministic formulation of the ensemble Kalman filter: an alternative to ensemble square root filters. *Tellus A*, 60(2):361–371.
- [37] Sakov, P. and Oke, P. R. (2008b). Implications of the form of the ensemble transformation in the ensemble square root filters. *Monthly Weather Review*, 136(3):1042–1053.
- [38] San, O. and Iliescu, T. (2015). A stabilized proper orthogonal decomposition reduced-order model for large scale quasi-geostrophic ocean circulation. *Advances in Computational Mathematics*, 41(5):1289–1319.
- [39] Stoica, P., Li, J., Zhu, X., and Guerci, J. R. (2008). On using a priori knowledge in space-time adaptive processing. *IEEE Transactions on Signal Processing*, 56(6):2598–2602.
- [40] Zhang, Y., Liu, N., and Oliver, D. S. (2010). Ensemble filter methods with perturbed observations applied to nonlinear problems. *Computational Geosciences*, 14(2):249–261.
- [41] Zhu, X., Li, J., and Stoica, P. (2011). Knowledge-Aided Space-Time Adaptive Processing. *IEEE Transaction on Aerospace And Electronic Systems*, 47(2):1325–1336.
- [42] Zubair, H. B. (2009). *Efficient Multigrid Methods based on Improved Coarse Grid Correction Techniques*. PhD thesis, Delft University of Technology, Netherlands.

Appendix A: Efficient Implementation of Stochastic Shrinkage

Ideally there should be no correlation between the forecast ensemble that we propagate with the physics-based model and the synthetic forecast ensemble that we generate. If we impose a block-diagonal structure of the transformation matrix

$$\mathcal{T}_i = \begin{bmatrix} \mathbf{T}_i & 0 \\ 0 & \mathcal{T}_i \end{bmatrix}, \quad (\text{A.1})$$

then, instead of equation (3.6), we search for separate transforms \mathbf{T}_i and \mathcal{T}_i for each ensemble such that:

$$\tilde{\mathbf{B}}_i^a = \gamma_i \mathcal{A}_i^f \mathcal{T}_i \mathcal{T}_i^\top \mathcal{A}_i^{f,\top} + (1 - \gamma_i) \mathbf{A}_i^f \mathbf{T}_i \mathbf{T}_i^\top \mathbf{A}_i^{f,\top}. \quad (\text{A.2})$$

Note that there is no unique solution to this equation.

Under the assumption that the synthetic ensemble is independent of the physical ensemble, but is transformed

through a standard ETKF formulation, it is the case that,

$$\mathcal{T}_i = \left(\mathbf{I} - \gamma_i \mathbf{Z}_i^{\text{f},\text{T}} \mathbf{S}_i^{-1} \mathbf{Z}_i^{\text{f}} \right)^{\frac{1}{2}}, \quad (\text{A.3})$$

where the formulation (2.6b) of \mathbf{S}_i uses all available information:

$$\mathbf{S}_i = \gamma_i \mathbf{Z}_i^{\text{f}} \mathbf{Z}_i^{\text{f},\text{T}} + (1 - \gamma_i) \mathbf{Z}_i^{\text{f}} \mathbf{Z}_i^{\text{f},\text{T}} + \mathbf{R}. \quad (\text{A.4})$$

This (almost uniquely) defines the transformation for the physical ensemble as,

$$\mathbf{T}_i = \left(\begin{array}{c} \mathbf{I} - (1 - \gamma_i) \mathbf{Z}_i^{\text{f},\text{T}} \mathbf{S}_i^{-1} \mathbf{Z}_i^{\text{f}} - \gamma_i \mathbf{A}_i^{\text{f},\dagger} \mathcal{A}_i^{\text{f}} \mathbf{Z}_i^{\text{f},\text{T}} \mathbf{S}_i^{-1} \mathbf{Z}_i^{\text{f}} - \gamma_i \mathbf{Z}_i^{\text{f},\text{T}} \mathbf{S}_i^{-1} \mathbf{Z}_i^{\text{f}} \mathcal{A}_i^{\text{f},\text{T}} \mathbf{A}_i^{\text{f},\text{T},\dagger} \\ - \frac{\gamma_i^2}{1 - \gamma_i} \mathbf{A}_i^{\text{f},\dagger} \mathcal{A}_i^{\text{f}} \mathbf{Z}_i^{\text{f},\text{T}} \mathbf{S}_i^{-1} \mathbf{Z}_i^{\text{f}} \mathcal{A}_i^{\text{f},\text{T}} \mathbf{A}_i^{\text{f},\text{T},\dagger} \end{array} \right)^{\frac{1}{2}} \quad (\text{A.5})$$

with \square^\dagger representing a pseudo-inverse (in this case we use the Moore-Penrose pseudo-inverse, keeping exactly $N - 1$ singular values of \mathbf{A}_i^{f}). In this case (A.5) comes from directly looking at all the terms of (goal-cov) expanded with (A.4), and by removing the terms found in (A.3).

This completes the optimized approach:

$$\begin{aligned} \mathbf{A}_i^{\text{a}} &= \mathbf{A}_i^{\text{f}} \mathbf{T}_i, \\ \mathcal{A}_i^{\text{a}} &= \mathcal{A}_i^{\text{f}} \mathcal{T}_i, \\ \bar{\mathbf{x}}_i^{\text{a}} &= \bar{\mathbf{x}}_i^{\text{f}} + \left(\gamma_i \mathcal{A}_i^{\text{a}} \mathbf{Z}_i^{\text{a},\text{T}} + (1 - \gamma_i) \mathbf{A}_i^{\text{a}} \mathbf{Z}_i^{\text{a},\text{T}} \right) \mathbf{R}_i^{-1} \mathbf{d}_i, \end{aligned} \quad (\text{A.6})$$

with the physical ensemble used to continue the computation defined as,

$$\mathbf{X}_i^{\text{a}} = \bar{\mathbf{x}}_i^{\text{a}} + \sqrt{N - 1} \mathbf{A}_i^{\text{a}}. \quad (\text{A.7})$$